Available online at www.sciencedirect.com

SCIENCE DIRECT

Developmental Biology 279 (2005) 402–419

DEVELOPMENTAL BIOLOGY

www.elsevier.com/locate/ydbio

Ephrin-As play a rhombomere-specific role in trigeminal motor axon projections in the chick embryo

Fabrice Prin, Keat-Eng Ng, Uma Thaker, Uwe Drescher, Sarah Guthrie*

MRC Centre for Developmental Neurobiology, 4th Floor New Hunt's House, King's College, Guy's Campus, London SE1 1UL, United Kingdom

Received for publication 27 August 2004, revised 20 December 2004, accepted 21 December 2004
Available online 22 January 2005

Abstract

In this study, we investigate the possible role of ephrin–Eph signaling in trigeminal motor axon projections. We find that *EphA* receptors are expressed at higher levels by rhombomere 2 (r2) trigeminal motor neurons than by r3 trigeminal motor neurons in the chick embryo. Mapping of rhombomere-specific axon projections shows that r2 and r3 trigeminal motor neurons project to different muscle targets, including the mandibular adductor and the intermandibularis muscles respectively. *Ephrin-A5* is expressed in these muscles, especially in some regions of the intermandibularis muscle, and can cause growth cone collapse of both r2 and r3 motor axons in vitro. We demonstrate that in vivo overexpression of *ephrin-A5* in the intermandibularis muscle, or overexpression of dominant-negative *EphA* receptors in trigeminal motor neurons leads to a reduction in branching of r3-derived motor axons specifically. Overexpression of full-length *EphA* receptors impairs the formation of r3 projections to the intermandibularis muscle. These findings indicate that ephrins and their Eph receptors play a role in trigeminal motor axon topographic mapping and in rhombomere 3-derived projections in particular.

Keywords: Ephrins; Eph receptors; Hindbrain; Trigeminal motor axons; Axon guidance; Chick

Introduction

Axon pathfinding during development depends on the presence of guidance cues in the environment through which axons grow (Dickson, 2002; Mueller, 1999). One important family of guidance molecules are the ephrins, comprising eight ligands, which bind a characteristic repertoire among fourteen Eph transmembrane tyrosine kinase receptors (reviewed by Frisen et al., 1999; Kullander and Klein, 2002; O'Leary and Wilkinson, 1999). Receptors of the A and B subclasses bind ligands of the A and B subclasses respectively, although EphA4 and EphB2 also bind B and A ephrins respectively (Himanen et al., 2004; Kullander and Klein, 2002). Ephrin–Eph receptor interactions play a role in a number of systems, including the mapping of retinal axons to correct target regions via a repulsive mechanism (reviewed in Frisen et al., 1999; Knöll and Drescher, 2002). Several studies have also implicated ephrins in the control of motor axon guidance and targeting in the spinal region, in particular for the innervation of the limb muscles by lateral motor column (LMC) neurons and the rostral somite by medial motor column (MMC) neurons (e.g. Eberhart et al., 2000, 2002, 2004; Helmbacher et al., 2000; Iwamasa et al., 1999; Kania and Jessell, 2003; Kilpatrick et al., 1996; Ohta et al., 1996).

We have previously reported that EphA receptors are expressed by cranial motor neuron subpopulations in the chick, while ephrins are expressed in the branchial arches (Küry et al., 2000). The expression of Eph receptors is not detected during the period in which axons are extending towards muscle anlagen in the branchial arches, but at and after stage 25, in the period when the muscle anlagen divide up into their component muscles (McClearn and Noden, 1988). Chemoattraction by HGF and other factors is likely to be involved in the initial projection of axons towards the branchial arches (Caton et al., 2000), but is unlikely to

* Corresponding author. Fax: +44 20 7848 6550.
E-mail address: sarah.guthrie@kcl.ac.uk (S. Guthrie).

0012-1606/$ - see front matter © 2005 Published by Elsevier Inc.
doi:10.1016/j.ydbio.2004.12.030

account for the later phase of specific mapping of axons to individual muscles. Our finding that EphA receptors are expressed at higher levels on rhombomere 2 (r2) trigeminal motor neurons than on r3 motor neurons (Küry et al., 2000) suggests that these receptor levels might determine r2 or r3-specific axon projections to their target muscles, *and/or* the topography of branching within individual muscles.

In the present study we have analyzed in detail the possible role of Eph–ephrins in these trigeminal axon projections. We have described *EphA* expression patterns in subpopulations of trigeminal motor neurons, and mapped the expression patterns of *ephrin-As* in the first arch muscles. We find that r2 and r3-derived trigeminal motor neurons project to distinct muscles, which express *ephrin-A5* in different patterns. In particular, the intermandibularis muscle, which receives projections from r3-derived motor neurons, contains regions of high and low level *ephrin-A5* expression. In vitro investigation showed that both r2 and r3 axons exhibited growth cone collapse in response to clustered ephrin-A5. Overexpression of *ephrin-A5* in the first branchial arch, or of dominant-negative *EphA* receptors in trigeminal motor neurons led to a loss of branching phenotype in r3-derived projections. This is consistent with the idea that ephrin-A–EphA signaling is involved in the topographic targeting of trigeminal axon projections, especially those derived from rhombomere 3.

Materials and methods

Preparation of embryos

Hens' eggs were incubated for 2–7 days and staged according to Hamburger and Hamilton (1951). Embryos were dissected in PBS and fixed for 2 h to overnight in 3.5% paraformaldehyde at 4°C. Embryos to be used for either in situ hybridization or immunohistochemistry on cryosections were washed in PBS, perfused with PBS/30% sucrose in a graded series and then embedded in OCT (BDH), frozen and cryosectioned at 20 μm. Embryos generated in viral overexpression experiments were treated in the same way.

In situ hybridization

Whole-mount in situ hybridization on normal or infected embryos was performed as published (Henrique et al., 1995) using *EphA3* and *EphA4* (Küry et al., 2000; kind gift of Dr. E. Pasquale), *ephrin-A5* (Drescher et al., 1995) and *MyoD* (Dechesne et al., 1994; kind gift of Dr. T. Braun) chick-specific probes. Some in situ hybridized whole-mounts were subsequently vibratome sectioned at 70 μm and immunostained.

For in situ hybridization on cryostat sections, slides were washed briefly in PBS and processed as described by Myat et al. (1996). The staining reaction was stopped in PBS/2 mM EDTA and the slides were mounted in Mowiol or processed for immunostaining after several washes in PBS.

Immunohistochemistry

Normal embryos were analyzed for trigeminal motor axon projections using whole-mount immunostaining. Some cryosections which had been in situ hybridized were subsequently immunostained. Some embryos infected with ephrin-A5 viral particles were fixed as above, subjected to in situ hybridization as whole-mounts and then processed for immunohistochemistry on vibratome sections.

Analyses of nerve projections and muscle development were performed on whole-mount preparations of longitudinally-hemisected heads and dissected lower jaws. The nomenclature of nerve branches is according to Kuratani and Tanaka (1990). First branchial arch muscles are named according to McClearn and Noden (1988). For the analysis of axonal projections on electroporated embryos, the hindbrain was dissected and stained separately from the corresponding hemisected head. Immunohistochemistry on cryostat sections (20 μm) was performed as in Chilton and Stoker (2000), and on vibratome sections as in Küry et al. (2000).

Primary antibodies used were anti-myosin (MF20) at 1:100 and anti-Islet1/2 (4D5) at 1:100 (both from the Developmental Studies Hybridoma Bank, University of Iowa), anti-neurofilament heavy chain (NF-H) at 1:800 (AB1991, Chemicon), polyclonal and monoclonal anti-GFP (1:250; Molecular Probes), anti-ephrin-A5 (1:10). Secondary antibodies used were Cy3-conjugated goat anti-mouse and FITC-conjugated goat anti-rabbit (Jackson Laboratories).

For whole-mount immunohistochemistry, embryos were fixed as above. After several washes in PBS/1% Triton X-100 (PTX), embryos were blocked overnight in PTX with 20% heat-inactivated sheep serum (HISS) and 0.02% sodium azide. Embryos were incubated in primary antibodies diluted in PTX, 20% HISS and 0.02% sodium azide at 4°C with rocking for 2–5 days, depending on the size of the tissue, then thoroughly washed in PTX for 36 h before the addition of secondary antibody in PTX, 20% HISS and 0.02% azide for 1–4 days at 4°C with rocking. After a final wash in PTX for 36 h, embryos were then cleared in graded dilutions of glycerol in PBS, before mounting in 90% glycerol/PBS with 2.5% DABCO (Merck). The largest samples were dehydrated in methanol and cleared in benzyl alcohol/benzyl benzoate (50:50).

Whole-mounts and immunostained cryosections were analyzed using epifluorescence microscopy (Nikon) or confocal microscopy (Biorad, Olympus).

Preparation of RCAS-ephrin-A5 virus and infection

RCAS(B)-ephrin-A5 (Dütting et al., 1999) and the control vector *RCAS(B)-AP* (Fekete and Cepko, 1993) were used to transfect chicken embryo fibroblasts (Morgan and Fekete, 1996). After 5 days of culture, the infection rate reached 100% as assessed using an anti-Gag antibody (Potts et al.,

1987). Culture medium containing retrovirus was harvested; concentrated viral stocks (10^6 to 10^7 infectious units/ml) were prepared as described by Fekete and Cepko (1993). Eggs were windowed and embryos (stages 17–20; embryonic day 3) were made accessible by removing the embryonic membranes. Concentrated viral stock was injected into the right first branchial arch and eggs were sealed with sellotape and reincubated for 3–4 days (to stages 28–29). Surviving embryos were removed and fixed as described. Some embryos were in situ hybridized for *ephrin-A5* as whole-mounts, then vibratome-sectioned and immunostained. Others were cryosectioned through the lower jaw and processed for immunostaining using anti-neurofilament, anti-ephrin-A5 and MF20 antibodies. The branching pattern was quantitated on confocal Z series images of infected and control sides of embryos using the Scion Image program. The number of pixels representing the branching pattern on infected sides was expressed as a percentage of the branching pattern on the uninfected side.

In ovo electroporation and transfection in chick embryos

Embryos at stages 10–13 were windowed and made visible using sub-blastodermal injection of India ink. Electroporation was performed as described previously (Guidato et al., 2003). For specific targeting of individual rhombomeres, electroporation was performed using flame-sharpened tungsten electrodes as described (Momose et al., 1999). For axon projection mapping, *pCAβlink-tau-GFP* (Guidato et al., 2003) was used. Embryos were viewed under epifluorescence after 24 h and the region of *GFP* expression was noted. For single rhombomere mapping studies, those not showing *GFP* expression in r2 or r3 alone were discarded. Embryos were then reincubated until embryonic day 6 and survivors were analyzed as above (see Immunohistochemistry section). After immunohistochemistry, whole-mount hindbrains were viewed under the confocal microscope for rhombomere-specific expression of GFP (green channel) into r2 or r3 against a background of Islet-1 (red channel). Dominant-negative *EphA3* and *EphA4* constructs (*pCAβ-EphA3Δ-IRES-myrGFP* and *pCAβ-EphA4Δ-IRES-myrGFP*) were made by sub-cloning *EphA4* cDNA truncated at position 1794 and *EphA3* cDNA truncated at position 1763 (Walkenhorst et al., 2000) in the Cla1 site of *pCAβ-IRES-myristylated GFP* (McLarren et al., 2003; kind gift of Dr. Andrea Streit). These truncations delete almost all of the cytoplasmic domain including the kinase domain and 1 of the 2 juxtamembrane tyrosines (*EphA4*) and including both of the juxtamembrane tyrosines (*EphA3*). In addition, the full-length *EphA3* cDNA was incorporated into the same expression vector. The empty vector *pCAβ-IRES-myrGFP* was used as a control. Electroporated embryos were reincubated until embryonic day 7 and processed for whole-mount immunohistochemistry as described above.

Quantitation of axon extension and branching was carried out on confocal Z series images by measuring the proximodistal distance within the intermandibularis muscle occupied by GFP-labeled projections in control and dominant-negative Eph receptor-expressing embryos. In each case, the length of labeled projections was expressed as a percentage of the total, neurofilament-labeled branching pattern, and a mean derived for each category of embryos.

Rhombomere explants

Rhombomere 2 (r2) or r3 explants for ephrin-A5-Fc staining or growth cone collapse assays were obtained from stage 22 chick embryos. Embryos were dissected in Hanks' balanced salt solution (HBSS) and the hindbrain was isolated from mesenchymal cells. Bilateral ventral portions of r2 or r3 were dissected using flame-sharpened tungsten needles, and kept on ice in HBSS. For ephrin-A5-Fc staining or growth cone collapse assays, explants were plated on glass coverslips coated with poly-L-lysine (Sigma; 20 μg/ml for 1 h to overnight at 37°C) and Laminin (Becton Dickinson; 20 μg/ml in PBS for 1–3 h at 37°C). All explants were cultured in medium consisting of 75% OptiMEM (Gibco) and 25% F12 (Gibco) supplemented with 5% fetal calf serum, 40 mM glucose, 1% penicillin/streptomycin, 10 ng/ml HGF (R&D Systems) and containing 4 mg/ml of methylcellulose (Sigma) for 2–3 days at 37°C in a humid atmosphere containing 5% CO_2.

Staining of explants with ephrin-A5-Fc fusion proteins

Explant cultures were blocked with medium containing 1 mg/ml BSA for 30 min at 37°C, washed with Ringer's solution then incubated for 1 h at 4°C in Ringer's solution containing 1 mg/ml of BSA and 10 μg/ml ephrin-A5-Fc (R&D Systems), or 10 μg/ml Fc protein. The cultures were then washed, fixed with 2% PFA for 10 min, washed again and incubated with Cy3-conjugated anti-human IgG (Fc-specific, Sigma) diluted 1:200 in Ringer's solution with BSA for 30 min at room temperature. After washing further, the explants were analyzed using epifluorescence microscopy.

Fig. 1. *EphA* and *ephrinA5* expression in the trigeminal nucleus at stages 24–25 and 28. (A) Diagram of chick embryo hindbrain showing positions of motor nuclei including the trigeminal nucleus (V). (B–C) Flat-mount hindbrain after immunohistochemistry for Islet-1/2, showing the localization of the cranial motor neurons at stages 24 (B) and 28 (C). The white lines in panel (B) indicate the rhombomere (r2 to r5) boundaries. The arrowheads in panel (C) indicate the two clusters of trigeminal motor neurons. fp: floor plate, V: trigeminal nucleus, VII: facial nucleus. (D, G, J) Expression of *EphA3* (D), *EphA4* (G) and *ephrin-A5* (J) mRNA detected by in situ hybridization on flat-mount hindbrains at stages 24–26. Arrowheads indicate trigeminal nuclei. (E, H, K) Expression of *EphA3* (E), *EphA4* (H) and *ephrin-A5* (K) mRNA detected by in situ hybridization on sections of flattened hindbrain through the trigeminal nucleus. (F, I, L) Same sections after immunodetection of Islet-1/2, showing the localization of trigeminal motor neurons. Floor plate (ventral) on the left, rostral at the top. Scale bar = 0.48 mm (B, C), 0.1 mm (E, F, H, I, K, L), 1 mm (D, G, J).

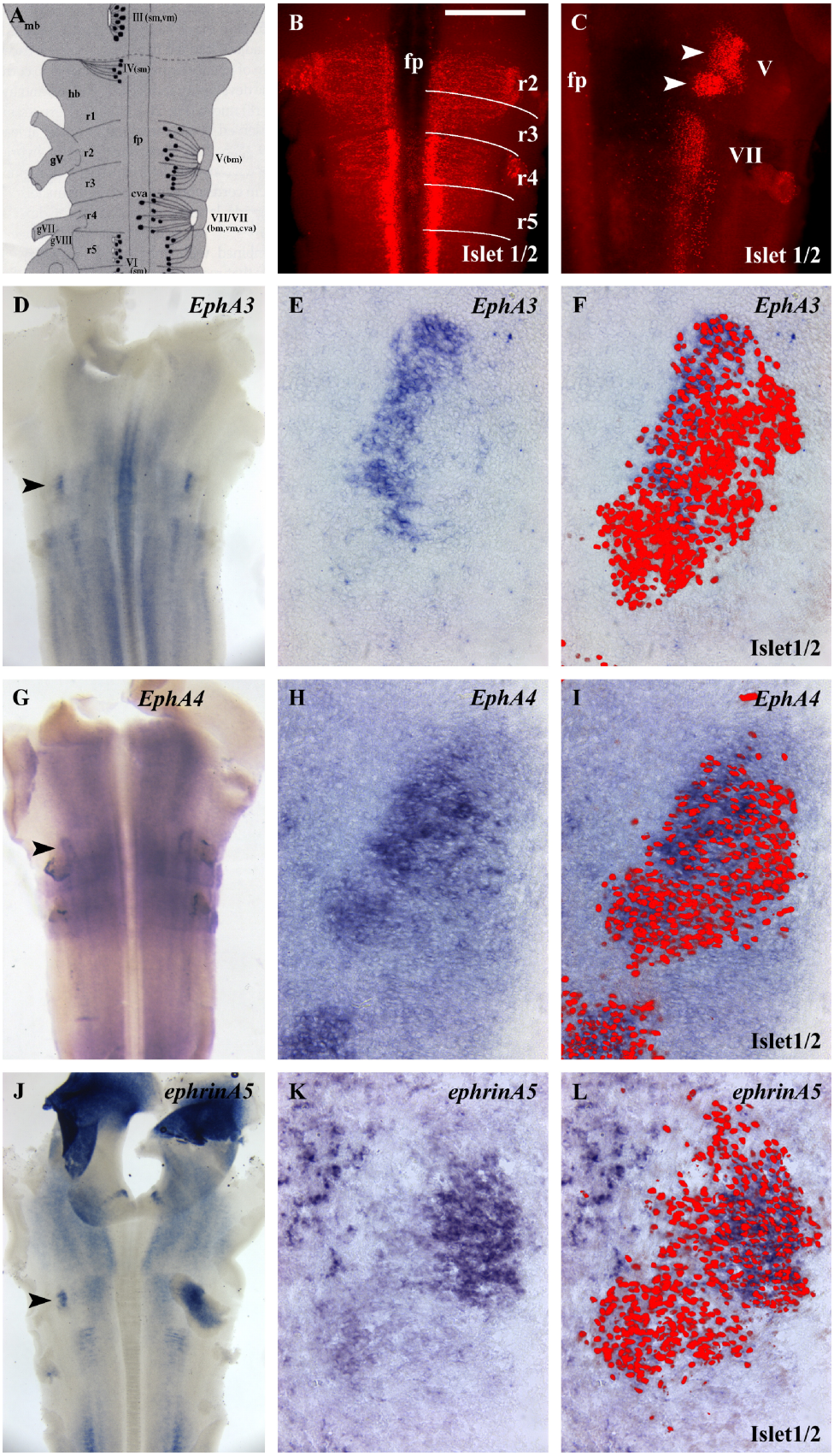
A
mb
III (sm,vm)
V(sm)
hb
r1
fp
gV
r2
V(bm)
r3
cva
r4
VII/VII
(bm,vm,cva)
gVII
gVIII
r5
VI
(sm)
B
fp
r2
r3
r4
r5
Islet 1/2
C
fp
V
VII
Islet 1/2
D
EphA3
E
EphA3
F
EphA3
Islet1/2
G
EphA4
H
EphA4
I
EphA4
Islet1/2
J
ephrinA5
K
ephrinA5
L
ephrinA5
Islet1/2

Growth cone collapse assay

Growth cone collapse assays were performed according to Vastrik et al. (1999), using ephrin-A5-Fc (R&D Systems; 100 μg/ml) or Fc protein as a control, in each case clustered using anti-human IgG (Fc-specific; Sigma) for 30 min at room temperature. Ephrin-A5-Fcs were added to the culture medium at a final concentration of 1 μg/ml and the explants were incubated for 30 min at 37°C, then fixed with pre-warmed 3.5% PFA and 10% sucrose for 20 min. Growth cones and axons were stained using TRITC-phalloidin (Sigma) at 1 μM and anti-neurofilament antibodies (AB1991; Chemicon) at 1:800 in PBS/1% Triton for 90 min at room temperature. After washing, the neurofilament antibodies were detected using FITC-conjugated anti-rabbit secondary antibodies. Explants were analyzed using epifluorescent microscopy. For each explant, total numbers of axons (individual and not bundles) were counted from the lateral explant borders, since previous data indicate that motor axons grow predominantly from lateral edges of such explants (Caton et al., 2000; Tucker et al., 1996). Numbers of growth cones with collapsed morphology were then counted and expressed as a percentage of total growth cone numbers for both control and ephrin-A5-Fc-treated explants.

Results

EphAs are expressed in specific subpopulations of trigeminal motor neurons

In the chick embryo, trigeminal motor neurons are born in ventral rhombomeres 2 and 3 (Lumsden and Keynes, 1989) and later migrate dorsally to take up positions close to their exit points (Simon et al., 1994, Figs. 1A–C). By stage 25, rhombomere boundaries have disappeared, and from stage 28 onwards, r2 and r3-derived neurons are subdivided into two discrete clusters (Figs. 1B, C). It is a feasible assumption that the rostral and caudal cluster are derived from r2 and r3 respectively (see later). Trigeminal motor axons project initially to the muscle plate of the first branchial arch, which later subdivides into a characteristic set of muscles (McClearn and Noden, 1988; Noden et al., 1999). By stage 25, trigeminal axons have reached the muscle plate and at stage 28 the nerve projection has divided into its component branches (see later).

In situ hybridization on whole-mount chick hindbrains at stages 25–26 using probes for *EphA3, EphA4* and *ephrin-A5* has shown a restriction of gene expression to rhombomere 2 (Figs. 1D, G, J; Küry et al., 2000). We analyzed expression of these genes in more detail, since these were the only EphA–ephrin-A family members known to be expressed by trigeminal motor neurons at stages when connections are forming (Küry et al., 2000). Further RNA in situ analysis at stages 28–29 was performed on coronal sections of hindbrain, together with immunostaining for Islet-1/2 to identify motor neurons (Tsuchida et al., 1994; Varela-Echavarría et al., 1996). *EphA3* expression was detected only within the r2 motor neuron cluster in a subset of medially-located neurons (Figs. 1E, F). *EphA4* showed a higher level of expression in the r2 cluster and a lower level of expression within the r3 cluster, with expression in both clusters predominantly located medially (Figs. 1H, I). *Ephrin-A5* also showed prominent expression in r2 but was detected at a lower level in r3, with a predominantly lateral rather than a medial localization (Figs. 1K, L). These data demonstrate that r2 neurons have higher levels of *EphA* and *ephrin-A* expression than r3 neurons at stage 25 and stage 28. It is possible that *EphA3/4* and *ephrin-A5* are expressed by largely non-overlapping populations of neurons, based on their respective medial and lateral localizations.

r2 and r3 trigeminal motor neurons have different muscle targets

To investigate the role of EphA–ephrin-A signaling in trigeminal motor axon pathfinding, we first documented the developmental relationship between the trigeminal motor neurons and their target muscles up to stage 29, using whole-mount double immunostaining for nerves and muscles, and confocal microscopy. At stage 25, the maxillomandibular branch of the trigeminal nerve (containing both sensory and motor axons) was detected as a single nerve trunk extending through the muscle mass that will eventually subdivide to give rise to the muscles of the adductor complex (compare schematic in Fig. 2A with Fig. 2B; McClearn and Noden, 1988). The most distal part of the maxillomandibular branch extends towards the midline in the proximal part of the lower jaw, forming the ramus circumflexus, which contacts the intermandibularis muscle (Figs. 2B, C; 4I). More MF20-positive myogenic cells were seen in the proximal part of this muscle than in the distal part (Figs. 2B, C). More proximally, sensory branches of the trigeminal nerve including the ramus mentalis are visible (Fig. 2B). At stages 27–28, hemisected preparations showed that the maxillomandibular nerve had branched extensively, giving rise to sensory branches in a distal to proximal sequence (Kuratani and Tanaka, 1990; Fig. 2D). The most distal branch, the ramus circumflexus, had arborized within the intermandibularis muscle (Fig. 2D). At stage 29, different orientations of the muscle fibers in the mandibular adductor complex suggest that the muscle mass is subdividing into the adductor externus, the pseudotemporalis and the pterygoideus (Fig. 2E; McClearn and Noden, 1988). In whole-mounts and vibratome sections, motor nerve branches to the adductor externus, pterygoideus, quadratus and pseudotemporalis muscles were identified (Figs. 2E–I). Innervation of the depressor palpebrae (Noden et al., 1999) was not observed in these preparations. At the same stage (29), the ramus circumflexus had formed further ramifications

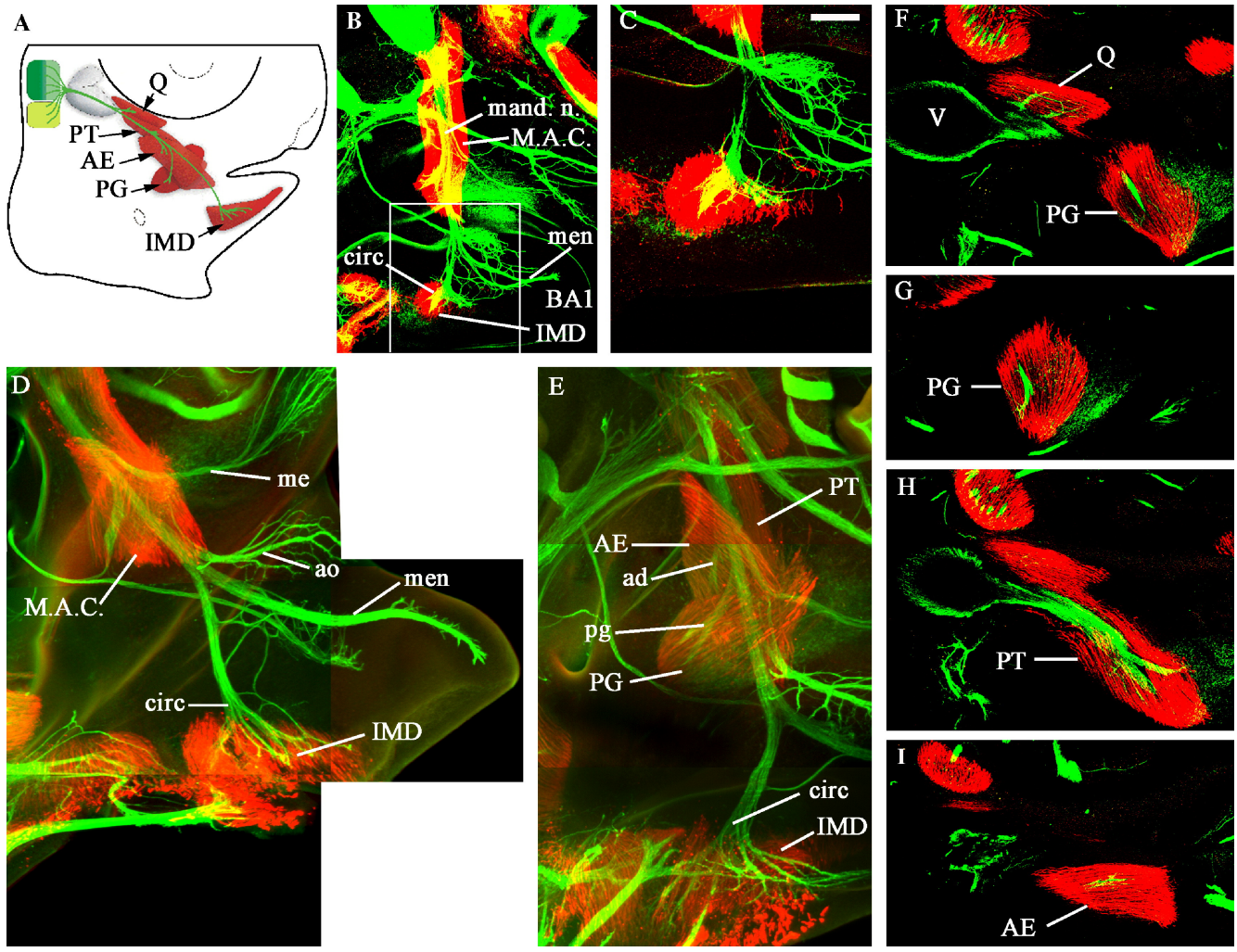

Fig. 2. Whole-mount immunostaining of muscles (red) and nerves (green) in the chick head. (A) Schematic diagram of chick head in lateral view, showing trigeminal motor innervation of the first branchial arch muscles at stage 29. Muscles are shown in red and nerve in green. Rhombomeres 2 and 3 shown in green and yellow respectively. (B–E) Lateral view of hemisected heads, stages 25 (B, C), 27–28 (D) and 29 (E). (C) Higher power view of the boxed area in panel (B). (F–I) Sagittal vibratome sections after nfh and MF20 immunostaining, showing the innervations of the first arch muscles at stage 28. Abbreviations for the trigeminal nerve branches: men: ramus mentalis, circ: ramus circumflexus, mand. n: mandibular nerve, me: ramus mandibularis externus, ao: ramus anguli oris, ad: adductor, pg: pterygoid innervations. Abbreviation for the first arch muscles: MAC: mandibular adductor complex, IMD: intermandibularis, AE: external adductor, PT: pseudotemporal, PG: pterygoideus, Q: quadratus. BA1: first branchial arch. Scale bar = 0.2 mm (B), 0.12 mm (D, E), 0.1 mm (C, F–I).

innervating the intermandibularis muscle branching extensively distally and medially towards the midline of the lower jaw (Figs. 2E, 4J).

To determine the muscle targets of r2 and r3 trigeminal motor neurons, we electroporated embryos at stage 10–13 with a *tau-GFP* construct allowing selective labeling of axons originating from electroporated neurons. Electroporation was targeted to either the r2 or the r3 region (confirmed by examination of embryos under epifluorescence after 24 h), and eggs were reincubated until stage 26–29, when embryos were harvested. The hindbrain was separated from the periphery of the head, including the pathways of the trigeminal nerve, and these two portions were processed separately. Hindbrains were stained with anti-Islet-1/2 and anti-GFP antibodies to visualize the electroporated neurons in relation to the entirety of the trigeminal nucleus, while peripheral portions of embryos were stained using anti-neurofilament and anti-GFP antibodies to determine which trigeminal nerve pathways were followed by r2 or r3-derived axons. For embryos targeted within r2 or r3 respectively at stage 10–13, we saw a corresponding restriction of GFP-labeled neurons to the rostral or caudal cluster of Islet-1/2-positive motor neurons within the trigeminal nucleus, supporting the idea that these are derived from specific rhombomeres. This suggests that the differences in *Eph* and *ephrin* expression described in the foregoing section is differential between specific rhombomere-derived motor neuron clusters.

For embryos in which GFP expression was restricted to r2 (Fig. 3A), 9/9 showed GFP-labeling of nerve projections to the mandibular adductor complex muscles (Figs. 3B, C, Table 1). In embryos that had reached stage 28 before

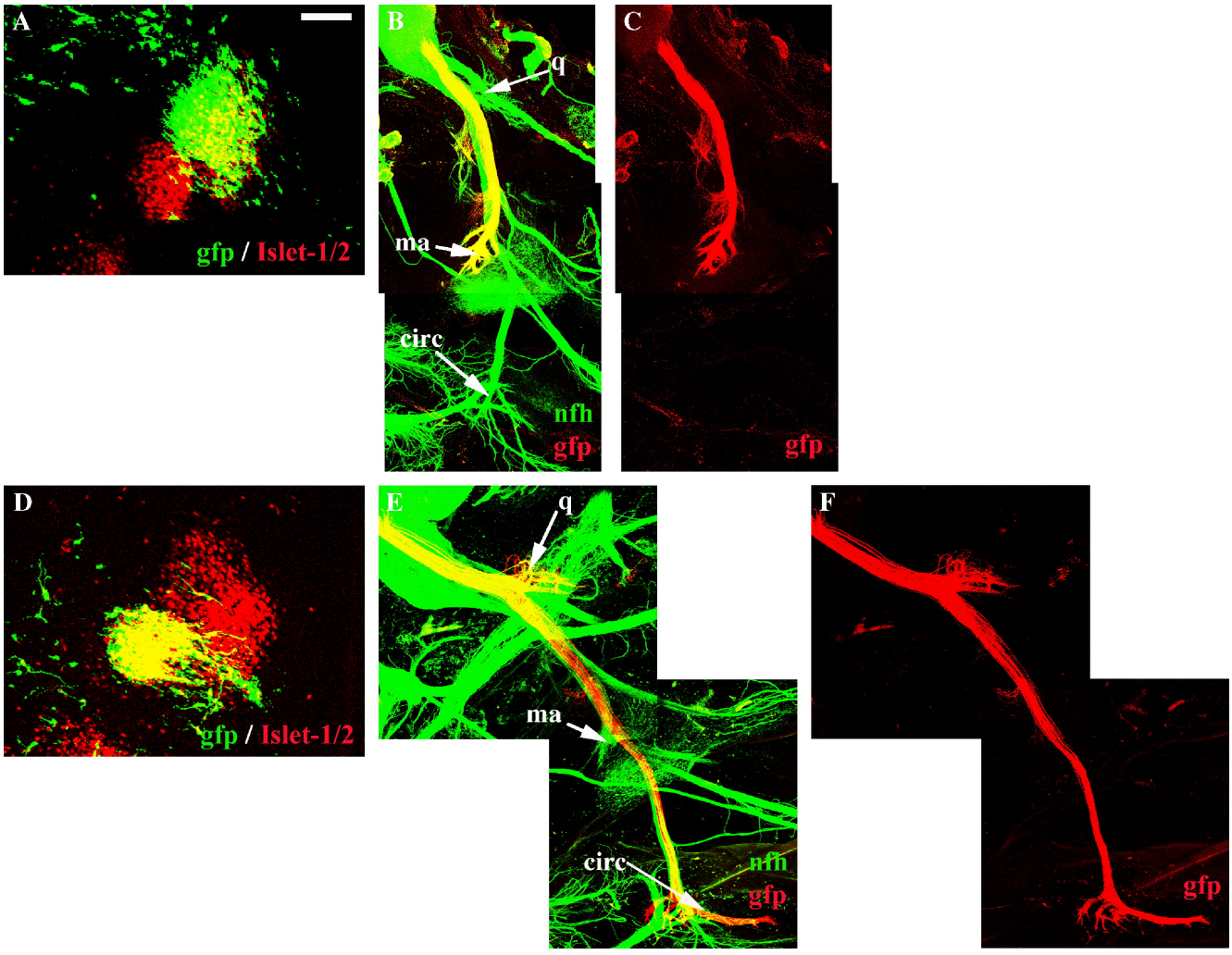

Fig. 3. Specificity of r2 and r3 motor axon projections. *Tau-GFP* was expressed in rhombomere 2 or rhombomere 3 by electroporation at day 2, and the embryos were incubated to E7. (A, D) Immunostaining for GFP (green) and Islet-1/2 (red) on flat-mounted E7 electroporated hindbrains, showing the restriction of GFP expression to the r2 (A) or r3 (D) cluster of trigeminal motor neurons. Floor plate is to the left, rostral at the top. (B, E) Whole-mount immunostaining for GFP (red) and neurofilament (green) on hemisected heads corresponding to the hindbrains show in panels (A) and (D) respectively. (B) The GFP-positive motor neurons shown in panel (A) project to the mandibular adductor complex. (E) The GFP-positive motor neurons shown in panel (D) project to the quadrate and intermandibularis muscles. (C) GFP as in panel (B), and (F) GFP as in panel (E), shown as single immunofluorescence. q: quadrate muscle innervations, ma: mandibular adductor innervation. Scale bar = 0.1 mm (A, D), 0.2 mm (B, C, E, F).

fixation, branching to innervate the adductor externus and the pterygoideus could also be distinguished (data not shown). By contrast, among embryos in which GFP expression was restricted to r3 (Fig. 3D), 8/11 cases showed GFP-labeled axons projecting to the quadratus and 11/11 showed projections to the intermandibularis muscle, with r3-derived axons branching throughout the proximodistal extent of the muscle (Figs. 3E, F; Table 1) in close correspondence with the neurofilament-labeled pattern. In one case, some axons corresponding to the pterygoideus branch were also GFP-labeled.

Table 1
Rhombomere-specific trigeminal axon tracing by GFP electroporation into rhombomeres 2 or 3

Axonal projection	Gfp expression in trigeminal motor neurons		
	Rhombomere 2 cluster: $n = 9$	Rhombomere 3 cluster: $n = 11$	Rhombomere 2 +3 clusters: $n = 13$
Quadratus	0	8	9
Mandibular adductor complex	9	1	12
Intermandibularis	0	11	13

Thus, trigeminal motor axons projecting from either r2 or r3 showed a distinctive and exclusive pattern of muscle innervation. In embryos which showed additional GFP labeling in the adjacent rhombomere (i.e. r2 and rostral r3 or r3 and caudal r2), there was a corresponding overlap of nerve projections between the two patterns (Table 1). Since there are six distinct muscle targets of the trigeminal nerve which are derived from the original first branchial arch

muscle mass (Noden et al., 1999), we might have expected to see a larger range of projections. However, our failure to observe these is likely to be explained by the fact that the full repertoire of trigeminal nerve muscle projections is not formed in the chick until around E10 (stage 36; McClearn and Noden, 1988; Warrilow and Guthrie, 1999). Our study was limited by the constraints of performing transfection at a timepoint when rhombomere boundaries were visible and analyzing at a timepoint when GFP expression persisted (up to 6 days in our hands) using whole-mount immunohistochemistry. Our observations show that trigeminal motor neurons which reside in r2 and r3 have distinct synaptic targets. The observation that the rostral and caudal neuronal clusters are derived from r2 and r3 respectively, taken together with our *EphA* expression data implies that trigeminal nerve branches to distinct muscles express different levels of EphA receptors.

Ephrin-As show patterned expression in trigeminal axon targets

In view of the expression of Eph receptors by specific subpopulations of trigeminal motor neurons, and the distinct axonal projection of r2 and r3 motor neurons, we next asked whether *ephrin-As* were expressed in the periphery of the head at times of nerve branching. Our previous data, obtained at stage 25–26, relied on the use of EphA-receptor bodies to detect ephrin-As in the developing head, and showed a strong localization within the midline of the developing lower jaw, in the region of the intermandibularis muscle (Küry et al., 2000). In situ hybridization revealed that *ephrin-A5* was expressed in the periphery. No expression of *ephrin-A2* was detected on first branchial arch muscles (data not shown).

In situ hybridization for *ephrin-A5* was performed on whole-mounts or on cryosections. At stage 28, vibratome sections showed that *ephrin-A5* was expressed in a V-shaped domain in the medial region of the lower jaw. Staining was strongest in the midline and in the proximal region adjacent to the pharynx (Fig. 4G). This staining pattern was similar to that previously obtained using EphA-Fc reagents on whole-mount lower jaws (Küry et al., 2000). Comparison with a *MyoD*-labeled vibratome section in the equivalent area showed that the *ephrin-A5*-expressing region corresponds with the region of the intermandibularis muscle (Fig. 4H). Comparison with nerve muscle staining in the same plane at stages 25 and 29, and with *MyoD* expression, showed that the strongest staining appeared to reside in a proximal region just outside the muscle mass, and in the raphe region joining the two sides of the muscle, which is devoid of nerve branches (see Figs. 4G–J). Muscle/nerve immunostaining on cryostat sections in situ hybridized for *ephrin-A5* at stage 26 similarly showed the localization of nerve and muscle in a region of low *ephrin-A5* expression (Figs. 4E, F); note that midline expression is not seen here due to the orientation of the section). Cryosections stained in the same way at the level of the adductor complex at stage 26 showed higher expression in the outer parts of the muscle mass away from the region of nerve branching (Figs. 4A–D, arrowheads). At stages 28–29, a similar localization of *ephrin-A5* staining was observed as at stage 25–26 (data not shown). Overall, both the intermandibularis and the adductor complex muscles expressed *ephrin-A5*, and nerve branches within these muscles tended to be located in regions of lower *ephrin* expression.

Overexpression of ephrin-A5 in the first branchial arch or of dominant-negative EphA receptors in the hindbrain leads to axon branching defects

To test the hypothesis that patterns of *ephrin-A* expression in the periphery of the developing head are involved in the guidance or topographic targeting of axon projections, we overexpressed ephrin-A5 ligands or dominant-negative EphA receptors in chick embryos in vivo. In the first approach, a replication-competent RCAS avian retrovirus encoding the full-length *ephrin-A5* was injected into the right first branchial arch of E3 (stage 17–20) chick embryos which were left to develop for 3–4 days (to stages 28–29). The lower jaws of these embryos were cryostat-sectioned and adjacent sections were immunostained with anti-neurofilament antibodies and either an anti-ephrin-A5-specific antibody or the MF20 antibody to localize the intermandibularis muscle. Alternatively, some embryos were in situ hybridized with an *ephrin-A5* probe, vibratome-sectioned and then immunostained with the anti-neurofilament antibody.

Immunofluorescence for ephrin-A5 revealed the ectopic, high-level expression of ephrin-A5 without revealing the endogenous low level expression (although expression was always detected in the optic tectum; data not shown). This is consistent with other data we obtained by in situ hybridization and immunohistochemistry showing that endogenous levels of *ephrin-A5* in the branchial arches were very low compared with other regions such as the optic tectum (data not shown). Ectopic ephrin-A5 expression was detected in the branchial arch, in the region of the developing intermandibularis muscle innervated by the ramus circumflexus (Fig. 5A). MF20-immunostaining showed that the morphology of this muscle was not perturbed by the ectopic ephrin-A5 overexpression (Fig. 5B). Merged confocal Z series of the pattern of neurofilament staining of the ramus circumflexus were compared for the control (uninjected) side of the embryo and the side which overexpressed ephrin-A5 (Figs. 5D, E). After reconstruction of the complete branching pattern of this muscle, we observed a reduction in branching of the nerve on the infected compared with the control side. The same result was obtained for three other embryos showing ectopic ephrin-A5 expression in the intermandibularis muscle ($n = 4$ in total). For a separate group of embryos in which whole-mount in situ hybridization showed ectopic ephrin-A5 expression in the intermandibularis region, a loss of nerve branches was also observed ($n = 3$). Thus, results from 7/7

embryos imply that axons respond to a high level of ephrin-A5 by repulsion or inhibition. To quantitate these changes in branching, we compared confocal Z series images of control and ephrin-overexpressing sides of 4 embryos by counting the total number of pixels representing the branching pattern in the intermandibularis muscle. This quantitation showed a mean reduction of 26% in the number of pixels on the side expressing the ephrin-A5 compared with the control side.

Our second approach to the in vivo role of Eph–ephrin interactions involved electroporation of a dominant-negative *EphA3* or *EphA4* (*EphA3Δ* or *EphA4Δ*) construct in the hindbrain. These constructs comprised a truncated form of the receptor lacking the cytoplasmic domain, which is known to act as a dominant-negative (Eberhart et al., 2004; Nishida et al., 2002; Walkenhorst et al., 2000; Yue et al., 2002), and an internal ribosome entry site followed by a myristylated GFP cDNA, allowing us to visualize the axonal projections of the targeted motor neurons. These constructs were targeted to r2 and/or r3 by electroporation at stage 10–13 and embryos were incubated until stages 26–29. As for embryos electroporated for mapping of axon projections, hindbrains and peripheral tissues from electroporated embryos were immunostained separately. Axons expressing the dominant-negative receptor were visualized by GFP immunostaining against a background of immunostained nerve pathways. Results that were obtained were essentially indistinguishable for embryos which misexpressed *EphA3ΔmyrGFP* or *EphA4ΔmyrGFP* dominant-negative constructs, and so the data will be discussed together. In cases of unilateral electroporation, the pattern of nerve branching, as revealed by neurofilament staining, was similar on both sides, with all nerve branches present. For embryos which expressed dominant-negative *EphA3Δ/A4ΔmyrGFP* in r2 motor neurons (Fig. 5G), no defects in axon pathfinding were observed, with nerve branches forming to the mandibular adductor complex (n = 42/42; Figs. 5H, I) as in embryos expressing *myrGFP* alone in r2 (n = 19/19; Table 2). When r3 was electroporated with a truncated Eph receptor, motor neurons still projected their axons to the intermandibularis muscle (n = 60/60; Figs. 5J–L) as in the control *myrGFP* embryos (n = 25/25; Table 2). GFP-labeled projections were noted for their presence within the proximal, medial or distal third of the ramus circumflexus arborization (Table 2). The axons expressing the dominant-negative receptor were restricted to the proximal portion (n = 30/60), or the proximal and medial portion (n = 28/60) of the intermandibularis muscle (Figs. 5C, F, J–L; Table 2) but were hardly ever detected in the distal region of this muscle (n = 2/60). Neurofilament-positive, GFP-negative axons, presumably representing the r3 motor neuron population which did not express the dominant-negative construct, innervated the remainder of the target region with a normal branching pattern (shown at higher magnification in Figs. 5C, F). In the case of electroporation of r3 motor neurons with a control vector expressing only the myristylated GFP (n = 23/25; data not shown; Table 2), no proximal restriction of GFP-positive axons was observed. Instead, projection patterns were indistinguishable from those obtained using vectors containing tau-GFP (Figs. 3D–F), with axons distributed throughout the proximodistal extent of the intermandibularis muscle.

There was some variability in the branching pattern of axons in embryos expressing the dominant-negative construct. Therefore, to provide further quantitation of the change in branching pattern, we measured the total length of the innervation pattern from proximal to distal within the intermandibularis muscle for *myrGFP* (control) axons compared with *EphA3ΔmyrGFP* or *EphA4ΔmyrGFP*-expressing axons. These measurements were done on a representative subset of embryos. For each embryo, the length of the innervation pattern was expressed as a percentage of the total branching pattern as visualized with anti-neurofilament antibodies, and a mean of these percentages was derived. We found that for control embryos (n = 12) the *myrGFP*-expressing axons extended along 93% of the length of neurofilament-positive branches within the muscle, whereas axons expressing dominant-negative Eph receptors extended along only 39.8% of the muscle length (n = 23). This clearly demonstrates a dramatic reduction in axon extension and branching among axons which expressed the dominant-negative constructs.

One explanation for this observation is that ephrin-A-mediated repulsion, dependent on ephrin-As expressed inside or outside the target area, is responsible for the characteristic extensive branching pattern of axons in the intermandibularis muscle. In particular, our observation of *ephrin-A5* expression proximal to the muscle region in normal embryos might imply that responses to this potentially repellent region might be required in order for axons to branch correctly within the muscle.

Overexpression of full-length EphAs impairs formation of r3 projections to the intermandibularis muscle

To test the significance of the higher levels of EphA receptors on r2 than on r3 trigeminal motor neurons, we overexpressed a full length *EphA3myrGFP* construct in the hindbrain and analyzed the resulting embryos in the same

Fig. 4. *ephrinA5* expression in the lower jaw. (A–F) *EphrinA5* mRNA detected by in situ hybridization on transverse cryosections through the jaw articulation (A–D) and the lower jaw (E–F) at stage 26 (rostral to caudal, distal part of the jaw on top). (B, D, F) same sections than panels (A, C, E) respectively, showing immunodetection of the muscles (red) and the nerves (green). (G) Transverse vibratome section through the lower jaw showing *ephrinA5* mRNA in situ hybridization at stage 28. (H) Transverse vibratome section through the lower jaw after *MyoD* mRNA in situ hybridization at stage 28, showing the position of the intermandibularis muscle. (I, J) Transverse view of stages 25 and 29 lower jaw, immunostained using MF20 (red) and anti-nfh (green) antibodies. Abbreviations as in Fig. 2. Scale bar = 0.1 mm (A, D), 0.25 mm (E, H), 0.15 mm, (I) 0.075 mm (J).

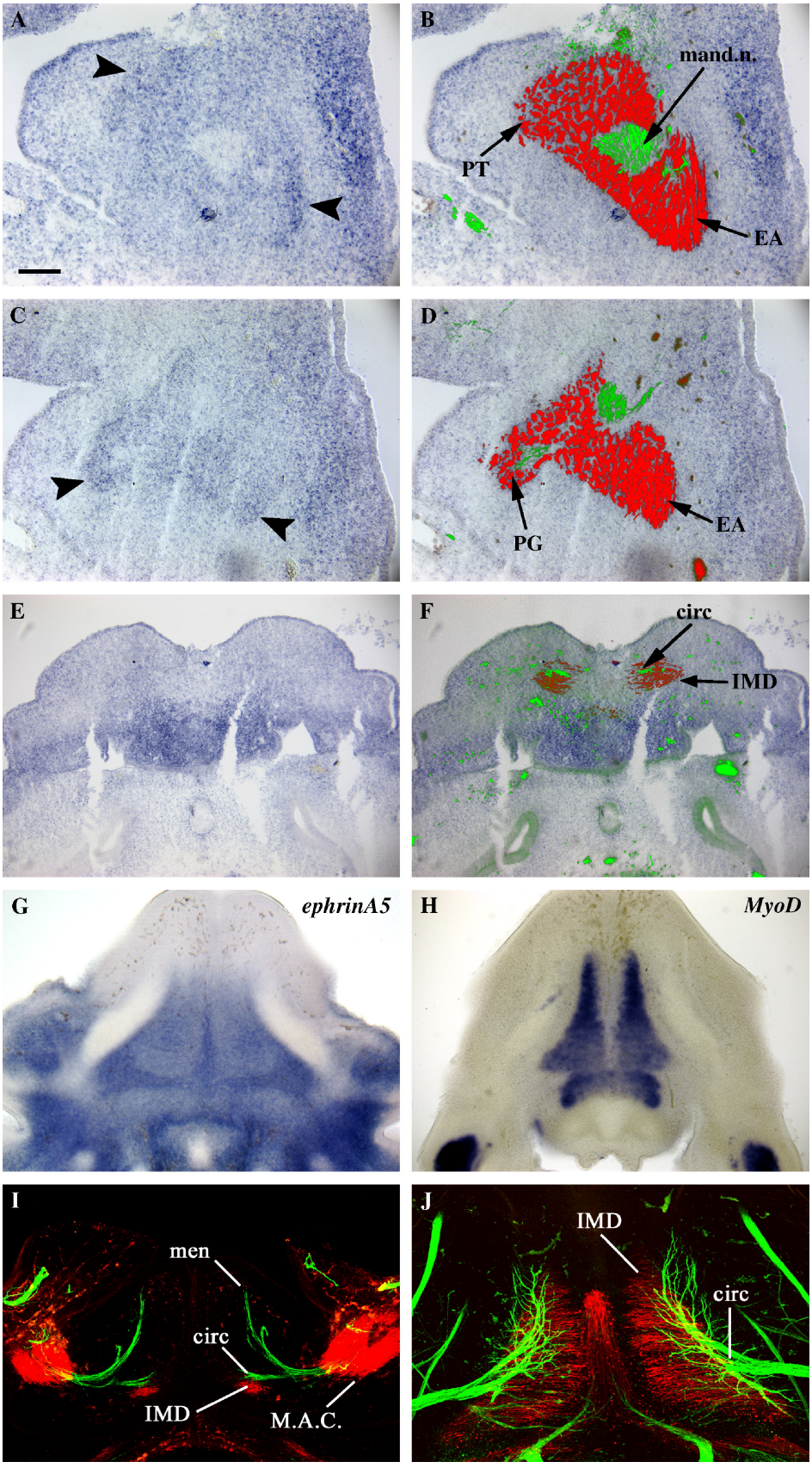
A
B
mand.n.
PT
EA
C
D
PG
EA
E
F
circ
IMD
G
ephrinA5
H
MyoD
I
men
circ
IMD
M.A.C.
J
IMD
circ

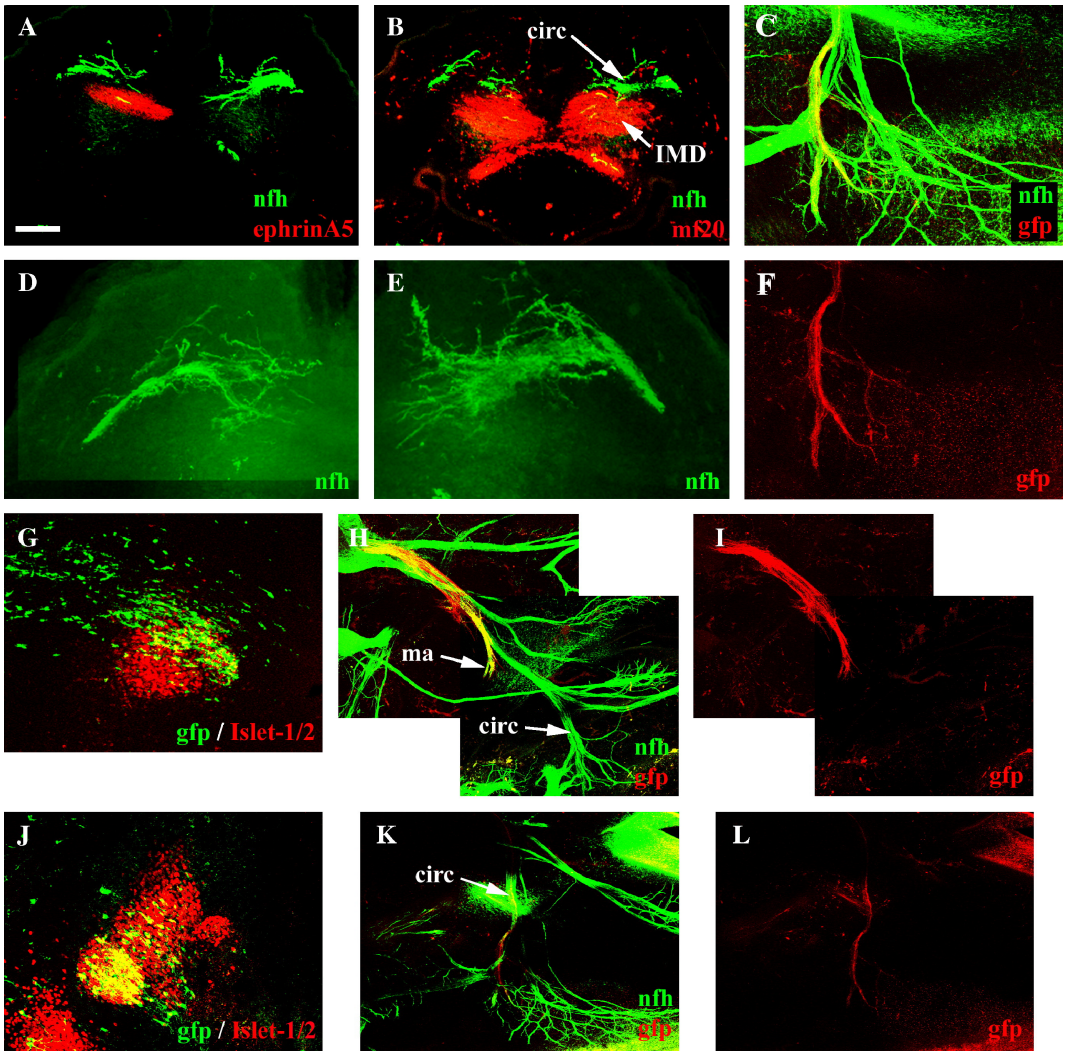

Fig. 5. Axon projections following overexpression of *ephrin-A5* or expression of dominant-negative *EphA* receptors. (A, B) Consecutive transverse sections through a stage 28 lower jaw after RCAS-ephrin-A5 infection at stage 18, immunostained for nfh (green), ephrin-A5 (red) (A) and MF20 (red) (B). (D, E) Merged Z series pictures of the intermandibularis innervation on the infected side (D) and on the control (uninfected) side (E). (G–L) *pCAβ-EphA4Δ-IRES-mGFP* was electroporated in r2 (G–I) and r3 (J–L) at stage 10 and embryos were incubated to stage 28. (C, F) Higher power views of nerve branching into intermandibularis muscle shown in panels (K) and (L) respectively, showing GFP (red) and anti-nfh (green). (G, J) Immunostaining for GFP (green) and Islet-1/2 (red) on flat-mounted electroporated hindbrains, showing the restriction of gfp expression to the r2 (G) or r3 (J). (H, K) Whole-mount immunostaining for GFP (red) and neurofilament (green) on hemisected heads corresponding to the hindbrains shown in panels (G) and (J) respectively. (I) gfp as in panel (H). (L) gfp as in panel (K). Scale bar = 0.3 mm (A, B), 0.15 mm (D, E), 0.2 mm (H, I, K, L), 0.1 mm (C, F, G, J).

way as described above. We wished to target expression predominantly to r3, to discover whether elevating EphA receptor levels in r3-derived trigeminal motor neurons would alter their axon pathfinding. However, in some cases, r2-derived neurons were also targeted. For embryos in which only r3 trigeminal neurons overexpressed *EphA3*, we found that axons projected only to the quadratus muscle (n = 5/5; Figs. 6G–I; Table 3), a normal r3 target. No GFP-labeled projections were seen extending to the intermandibularis muscle, despite the appearance of neurofilament-

Table 2
Projection of GFP-positive axons in embryos expressing dominant-negative Eph receptors

	MAC innervation	IMD proximal	IMD proximal + medial	IMD distal + medial + distal	Total
EphA3Δ/A4Δ-myrGFP in R2	42	0	0	0	42
EphA3Δ/A4Δ-myrGFP in R3	0	30	28	2	60
myrGFP in R2	19	0	0	0	19
myrGFP in R3	0	0	2	23	25

Abbreviations: MAC—mandibular adductor complex, IMD—intermandibularis.

labeled projections in this region. This probably indicates the projection of non-GFP-labeled r3-derived neurons to their normal target muscle. When both r2 and r3 neurons were targeted, however, GFP-labeled axons extended to the mandibular adductor complex in addition to the quadratus (n = 9/9; Figs. 6A–F; Table 3). Taken together with the data from r3 targeted expression alone, this is likely to reflect the projection of r2-derived neurons to their correct MAC target muscles. Thus, overexpression of full-length EphAs does not impair the formation of r2-derived axon projections, but specifically impairs r3-derived projections to the interman-dibularis muscle.

Table 3
Projection of GFP-positive axons in embryos expressing full-length *EphA3* receptors

	Quadratus innervation	MAC innervation	IMD innervation
EphA3-myrGFP in R3 (n = 5)	5	0	0
EphA3-myrGFP in R3 and R2 (n = 9)	9	9	0

Abbreviations: MAC—mandibular adductor complex, IMD—intermandi-bularis.

Trigeminal motor axons show growth cone collapse in the presence of ephrin-A5 in vitro

To test the sensitivity of trigeminal motor axons to ephrins in vitro, we performed growth cone collapse assays. Application of preclustered ephrin-As to retinal ganglion neurons in vitro have previously been used to investigate the responses of neurons to ephrin ligands in systems in which in vivo gradients of ephrins may play a role in topographic mapping (e.g. Drescher et al., 1995). To test the effects of ephrins on trigeminal motor axons, we plated explants consisting of the ventral two-thirds of the hindbrain from r2/3 levels of stage 22 chick embryos (Fig. 7A) on poly-L-lysine/laminin coated substrata. After 2–3 days in culture, extension of axons was observed to occur predominantly from the lateral borders of explants on to the laminin-coated substrata (Fig. 7B). Previous data from collagen gel cultures of both chick and rat tissues have shown that motor axons extend from the lateral borders of such hindbrain explants (Caton et al., 2000; Tucker et al., 1996). Axons were tipped with expanded growth cones (Figs. 7G–I). We first stained these explants using ephrin-A5-Fc "ligand-body" reagents to detect Eph receptors on axons. Axons originating from both r2 and r3 levels showed positive staining with this

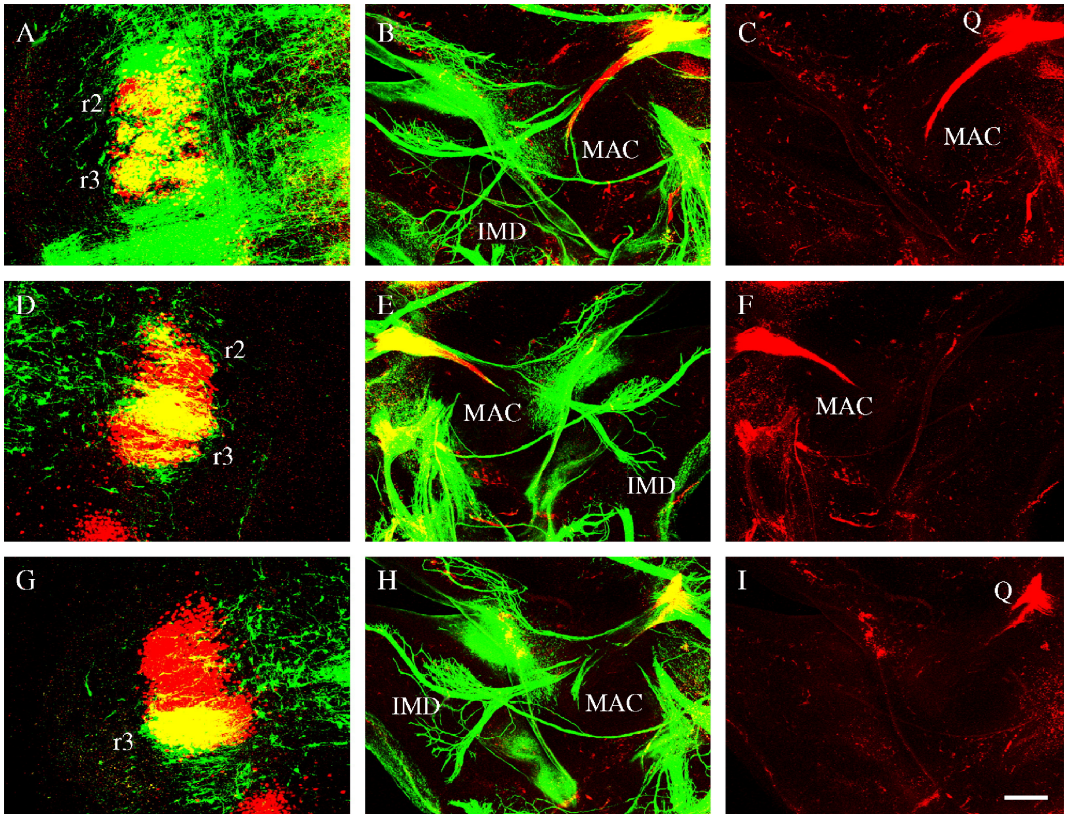

Fig. 6. Axon projections following overexpression of full-length *EphA3* receptors. (A–I) *pCAβ-EphA3-myrGFP* was electroporated in r2 and r3 (A–F) or r3 (G–I) at stage 10 and embryos were incubated to stage 28. (A, D, G) Immunostaining for GFP (green) and Islet-1/2 (red) on flat-mounted electroporated hindbrains, showing GFP expression in r2 and r3 (A, D) and r3 only (G). (B, E, H) Immunostaining on whole-mount heads for GFP (red) to show electroporated neurons and anti-nfh (green) to show entirety of nerve projections. (C, F, I) Same preparations as in panels (B), (E) and (I) respectively but showing GFP only. Scale bar = 0.1 mm (A, D, G) and 0.2 mm in all remaining panels.

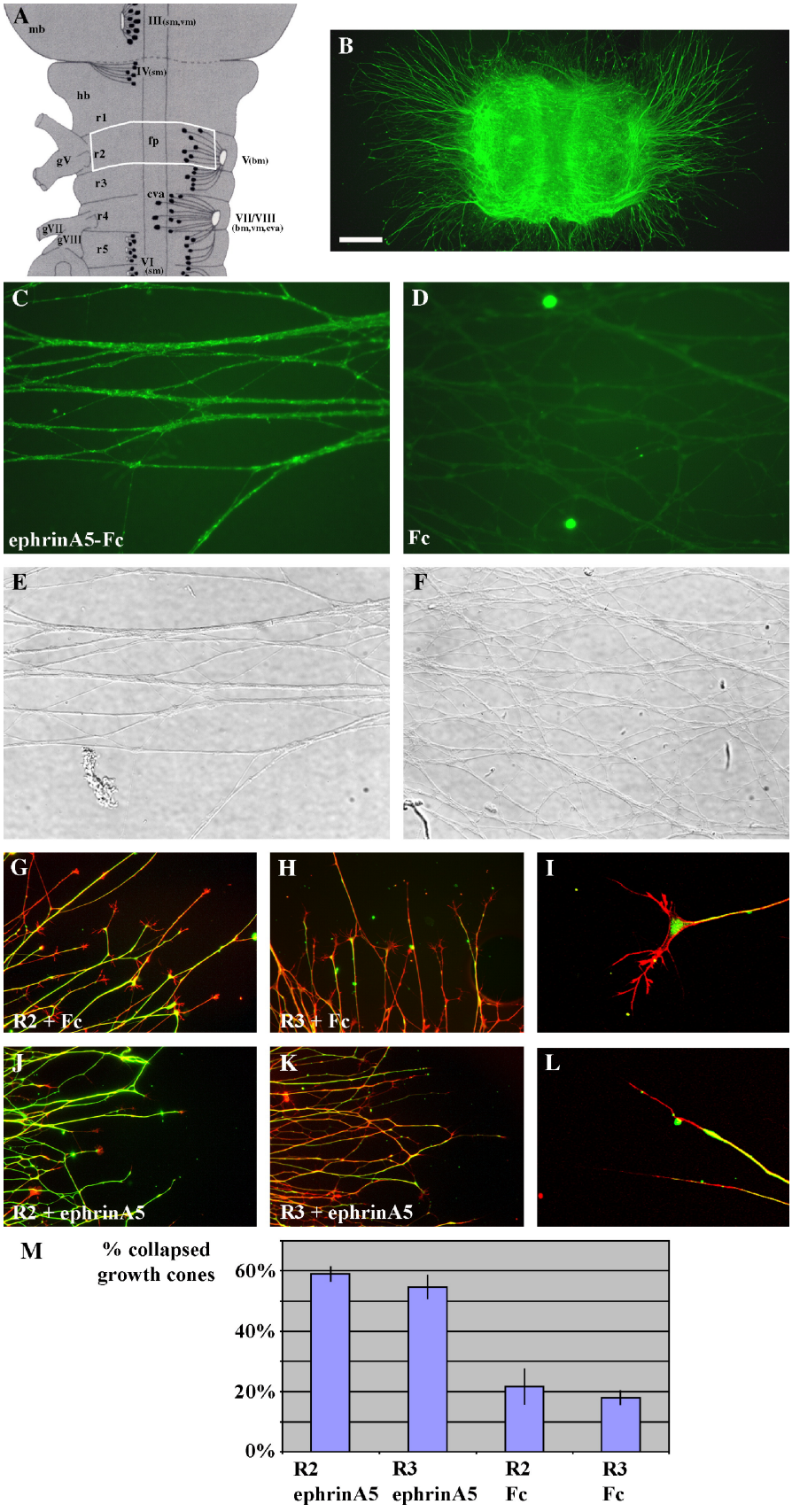
A
mb
III(sm,vm)
IV(sm)
hb
r1
fp
r2
gV
V(bm)
r3
cva
r4
gVII
gVIII
VII/VIII
(bm,vm,cva)
r5
VI
(sm)
B
C
ephrinA5-Fc
D
Fc
E
F
G
R2 + Fc
H
R3 + Fc
I
J
R2 + ephrinA5
K
R3 + ephrinA5
L
M
% collapsed
growth cones
60%
40%
20%
0%
R2
ephrinA5
R3
ephrinA5
R2
Fc
R3
Fc

reagent, in comparison with no staining using control Fc reagents (Figs. 7C–F). This confirms that trigeminal r2 and r3 motor axons, which express mRNAs encoding Eph receptors in vivo, also express Eph receptors on their surfaces in such a culture system. However, we were unable to detect different levels of Eph receptors using this method, although it might be expected that r2 axons would contain higher concentrations of Eph receptors than r3 axons.

We compared anti-neurofilament immunostaining (to detect axon shafts) and phalloidin (to detect filamentous actin in growth cones) in explants treated with a clustered Fc reagent alone (control), compared with those treated with a clustered ephrin-A5-Fc reagent. In control explants, the majority of neurons bore expanded growth cones and only a minority showed growth cone collapse (21% and 18% for r2 and r3 respectively; Figs. 7G, H, I, M). By contrast, explants treated with the preclustered ephrin-A5-Fcs showed the majority of growth cones with collapsed morphology (Figs. 7J–M). Such growth cone collapse was observed for 58% of r2 neurons and 54% of r3 neurons (Fig. 7M). These data indicate that both r2 and r3 trigeminal motor neurons respond to the application of exogenous ephrins by cytoskeletal collapse.

Discussion

Our major findings in this study are, firstly, that trigeminal motor neurons resident in r2 or r3 express high and low levels of *EphAs* respectively. Secondly, r2 and r3-derived trigeminal motor neurons project to distinct muscles in the first branchial arch, which express *ephrin-A5* in different patterns. Thirdly, trigeminal motor axons exhibit growth cone collapse in response to applied ephrins. Fourthly, overexpression of ephrins in the trigeminal target field, or of dominant-negative Eph receptors on motor axons leads to axon branching defects of r3 neurons, consistent with ephrins playing a repulsive role in their topographic projection patterns inside their muscles target. Finally, overexpression of full-length EphAs in trigeminal motor neurons impairs the formation of r3 projections to the intermandibularis muscle, implying that low levels of EphA expression are required for this projection.

Rhombomere 2-derived motor neurons express higher levels of EphA receptors

Our analysis of the expression patterns of *EphA* receptors in trigeminal motor neurons together with single rhombomere GFP-labeling suggests that r2 axon projections to the mandibular adductor complex have higher levels of EphA receptors than r3 projections to the intermandibularis muscle. The differential expression of EphAs on r2/r3 motor neurons is detected only after the axons have reached their target muscles, implying a role in branching. At stages 28–29, the expression of *EphA3/A4* appeared restricted to a medial subset of motor neurons, while *ephrin-A5* was expressed mainly by a lateral subset; however, the precise degree of overlap remains to be determined. In the retinotectal system, co-expression of ephrin ligands with EphA receptors on the nasal retinal ganglion cell population was found to lead to desensitization of axons to exogenously applied ephrin ligands (Hornberger et al., 1999). It is possible that the same holds here, since in in vivo experiments, only r3-derived trigeminal axons were found to respond conspicuously to overexpression of ephrins or of dominant-negative Eph receptors. While in vitro assays showed that both r2 and r3 axons collapsed their growth cones in response to ephrin-As, it is possible that r2 and r3 axons might respond to different levels of ephrin-A ligands, in a manner which is not revealed by exposure to a uniform concentration of ligands applied in the medium. This sensitivity might be modulated by the co-expression of ephrin-As.

R2 and R3 contain different motor pools

Here, we demonstrate that in the chick embryo, r2 and r3 trigeminal motor neurons have different synaptic targets, i.e. house different motor pools. These data are consistent with previous studies showing a zonation of motor pools within the trigeminal motor nucleus in the adult pigeon (Wild and Zeigler, 1980) and r3 rhombomere reversal experiments, in which axons consistently showed a preference for innervation of particular first branchial arch muscles (Warrilow and Guthrie, 1999). Rhombomere fate maps in the chick embryo also showed that rostral and caudal parts of the trigeminal motor nucleus derived from r2 and r3 respectively (Marin and Puelles, 1995). In a transgenic zebrafish expressing *GFP* under an *Islet-1* promoter, there was differential innervation of targets by r2 and r3 neurons. While r2 neurons innervated the adductor mandibulae, r3 neurons innervated the anterior and posterior intermandibularis muscle (Higashijima et al., 2000). These muscles are homologues of the mandibular adductor and intermandibularis muscles in the chick, consistent with the phylogenetic conservation of the innervation pattern of the trigeminal nerve (Song and Boord, 1993).

It seems likely that this projection pattern is intrinsically programmed by rhombomere-specific factors, which might

Fig. 7. Growth cone collapse assay. (A) Schematic drawing showing the area dissected for rhombomere explants (example of r2). (B) Anti-nfh staining on r2 explant after 3 days in vitro. (C) Ephrin-A5-Fc staining on r2/r3 explant showing axonal staining, with corresponding bright field image (E). (D) Fc staining on r2/r3 explant control, with corresponding bright field image (F). (G, H, I) Anti-nfh/phalloidin staining on Fc-treated r2 (G, I)/r3 (H) explant. (J–L) Anti-nfh/phalloidin staining on Ephrin-A5-Fc-treated r2 (J, L)/r3 (K) explant. Scale bar = 300 μm (B), 26 μm (C–F), 77 μm (G, H, J, K), 20 μm (I, L). (M) Histogram showing incidence of growth cone collapse among neurons growing from r2 or r3 explants treated with ephrin-A5 (first two bars) or with control Fcs (third and fourth bars). The data correspond to the mean of 3 independents experiments, the total numbers of axons counted are: 641 for R2 ephrinA5, 394 for R3 ephrinA5, 354 for R2 Fc, 369 for R3 Fc.

also dictate the higher level of *EphA3/A4* expression in r2. A promising candidate to confer r2 identity is *Hoxa2* which is expressed in both r2 and r3 in the chick (Prince and Lumsden, 1994), while *Hoxb2* is expressed in r3 and not r2 (Wilkinson et al., 1989) and might govern r3 identity. It is interesting to note that in the spinal region, *EphA4* expression and dorsal motor axon projections to the limb are under the control of the LIM transcription factor Lim1 (Kania and Jessell, 2003; Kania et al., 2000). However, no expression of Lim1 is detected in the chick hindbrain at the relevant stages (Varela-Echavarría et al., 1996).

Ephrin-A5 causes trigeminal motor neuron growth cone collapse

The higher expression levels of EphAs on r2 axons might predict an enhanced response to ephrins, and yet we found that ephrin-A5 applied either in the medium caused growth cone collapse of both r2 and r3-derived trigeminal motor axons. By comparison, in the retinotectal system, posterior and not anterior tectal membranes were inhibitory and repellent for temporal but not nasal axons (Walter et al., 1987a, b). Candidates for this posterior repellent activity are ephrin-A5 and ephrin-A2, but while the former induces collapse and repulsion of both temporal and nasal axons (Drescher et al., 1995), the latter is specific for temporal axons (Monschau et al., 1997). However, when lower concentrations or gradients of ephrin-A5 are applied, nasal axons lose responsiveness first, reflecting a higher sensitivity of temporal axons to this molecule (Monschau et al., 1997; Rosentreter et al., 1998). In our system, application of graded concentrations of ephrins might be required to reveal differences in sensitivity. In preliminary in vitro experiments utilizing lower concentrations of ephrins, we found that r2-derived axons manifest an increased tendency for growth cone collapse relative to r3-derived axons (data not shown).

In vivo overexpression of ephrin-A5, dominant-negative EphA receptors or full-length EphA receptors disrupts the formation of r3-specific projections

Overexpression of either ephrin ligands or truncated Eph receptors on the target field or the trigeminal motor axons respectively, yielded a loss of branching phenotype of the r3-derived ramus circumflexus which innervates the intermandibularis muscle. This response of r3-derived motor neurons, which express lower Eph levels, to expression of dominant-negative receptors, is consistent with that in the visual system, in which expression of dominant-negative EphA4 reduces ephrin responsiveness of the axonal population with lower Eph levels, i.e. the nasal axons (Walkenhorst et al., 2000). In our case, this may suggest either that r3 neurons are more reliant on ephrin guidance cues than r2 neurons, or that expression of a dominant-negative receptor has a more dramatic effect in attenuating Eph-mediated signaling for this population.

Our findings appear at first glance contradictory in that both overexpressions of ligand and of dominant-negative receptors give the same phenotype. This situation may arise due to the fact that ephrin-A5 appears to be localized in a region proximally within the lower jaw (see Fig. 8) and along the midline raphe. Branching of axons into the intermandi-

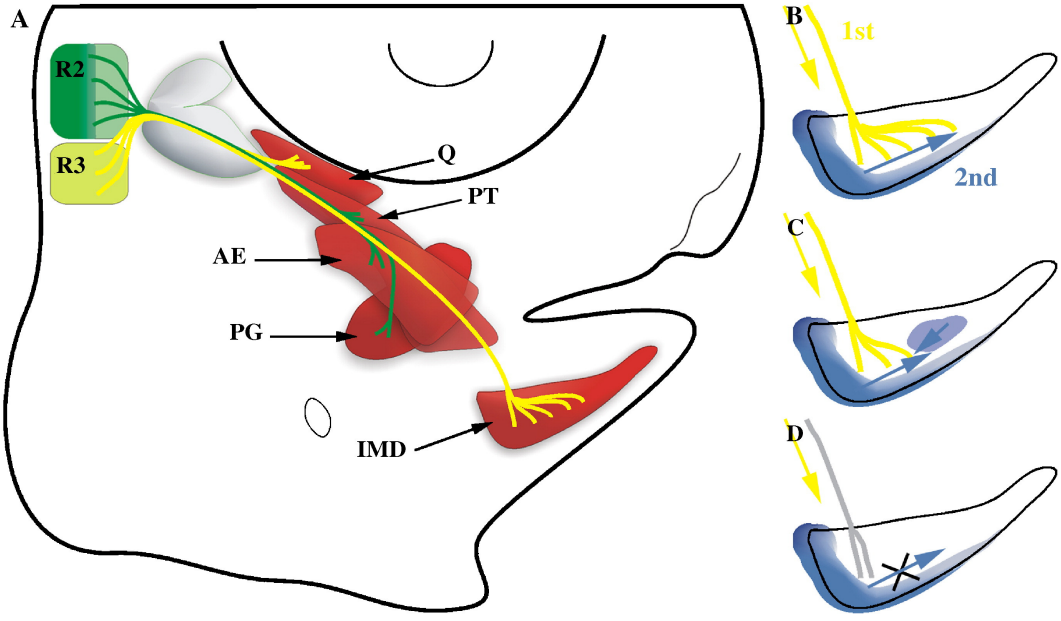

Fig. 8. R2 and R3 trigeminal motor neuron projections and phenotypes obtained after perturbation of EphA–ephrin-A signaling. (A) Trigeminal motor axon projections. (B) 1st: Chemoattraction towards the proximal part of the first branchial arch. 2nd: Proximal to distal repulsion by ephrin-A5 leads to branch formation toward the distal region. (C) Overexpression of ephrin-A5 prevents branch formation. (D) Abrogation of ephrin–Eph signaling prevents the repulsion necessary for distal branching to occur.

bularis muscle might then occur due to repulsion from proximal to distal, causing branches to form in this direction. Overexpression of ephrin-A5 in the middle of this region would prevent branch formation, while abrogation of ephrin–Eph signaling would prevent the proximal to distal repulsion necessary for branch formation to occur (Fig. 8).

Experiments in which high levels of EphA receptors were expressed in r3 or r2 and r3 neurons further confirmed the sensitivity of r3-derived axon projections to levels of EphA expression. We had anticipated that r3 projections might be transformed into an r2 phenotype by this manipulation, but this was not the case. Instead, r3 projections to the intermandibularis muscle failed to form, although those to the quadratus, another r3 target, were intact. The failure of r3 axons to project to the intermandibularis muscle is unlikely to be non-specific, since projections (presumably) from r2 neurons to their mandibular adductor targets formed normally. The most likely interpretation of this result is therefore that higher levels of EphA receptors confer upon these axons sensitivity to the low concentrations of ephrins found in proximal regions of the lower jaw, for example in the environs of the mandibular adductor complex (see Figs. 4A–D). This is consistent with our results from preliminary in vitro experiments using lower concentrations of ephrins, in which r2-derived neurons showed an increased tendency to exhibit growth cone collapse relative to r3-derived neurons. r2 neurons might possess additional mechanisms allowing them to avoid inappropriate (r2) muscle targets.

Conclusions and future prospects

At first glance, ephrin–Eph interactions seem to play a different role in the trigeminal–branchial arch system than in the projections of spinal motor neurons into the limb. In the latter system, Eph receptors (and ephrins) are expressed on lateral motor column (LMC) neurons as they select dorsal or ventral limb territories, and on medial motor column (MMC) neurons as they project towards the epaxial muscles (reviewed by Eberhart et al., 2004; Palmer and Klein, 2003). EphA4 expression is crucial for the innervation of lateral LMC neurons of the dorsal limb via a repulsive mechanism (Eberhart et al., 2002; Helmbacher et al., 2000; Kania and Jessell, 2003). However, for medial MMC neurons which project epaxially, EphA4 appears to mediate positive interactions and ectopic expression of ephrins in the caudal sclerotome allows MMC axons to aberrantly enter this region (Eberhart et al., 2004). By contrast, the primary extension of trigeminal axons into the branchial arch field may be under the control of diffusible factors (Caton et al., 2000), with the onset of Eph receptor expression occurring once the first arch muscle mass has been reached (Küry et al., 2000; this study). Eph–ephrin interactions are therefore implicated in topographic mapping of motor axon projections to muscles as they subdivide, with axons expressing higher concentrations of Eph receptors projecting to the proximal arch muscles and vice versa. Our data from overexpression of EphAs are consistent with this interpretation, while data from overexpression of ligands or truncated receptors are more suggestive of a role in branching within the intermandibularis muscle. A more critical examination of the idea that different ephrin levels from proximal to distal determine trigeminal axon branching into muscles would require analysis at all intermediate stages of subdivision of the muscle mass. In both the trigeminal and the limb system, the significance of co-expression of ephrins and Eph receptors on motor axons remains unclear, but might be involved in axon–axon interactions as well as those with the mesenchymal environment. More detailed knowledge of the molecular interactions of Ephs and ephrins in *cis* and in *trans* on different axonal subtypes will be required to understand the significance of receptor and ligand co-expression.

Acknowledgments

We thank Jon Gilthorpe for provision of pCAβlink, Andrea Streit for pCAβ-IRES-myrGFP and Bernd Knöll for advice on tissue culture.

References

Caton, A., Hacker, A., Naeem, A., Livet, J., Maina, F., Bladt, F., Klein, R., Birchmeier, C., Guthrie, S., 2000. The branchial arches and HGF are growth-promoting and chemoattractant for cranial motor axons. Development 127, 1751–1766.

Chilton, J.K., Stoker, A.W., 2000. Expression of receptor protein tyrosine phosphatases in embryonic chick spinal cord. Mol. Cell. Neurosci. 16, 470–480.

Dechesne, C.A., Wei, Q., Eldridge, J., Gannoun-Zaki, L., Millasseau, P., Bougueleret, L., Caterina, D., Paterson, B.M., 1994. E-box- and MEF-2-independent muscle-specific expression, positive autoregulation, and cross-activation of the chicken MyoD (CMD1) promoter reveal an indirect regulatory path. Mol. Cell. Biol. 14, 5474–5486.

Dickson, B.J., 2002. Molecular mechanisms of axon guidance. Science 298, 1959–1964.

Drescher, U., Kremoser, C., Handwerker, C., Loschinger, J., Noda, M., Bonhoeffer, F., 1995. In vitro guidance of retinal ganglion cell axons by RAGS, a 25 kDa tectal protein related to ligands for Eph receptor tyrosine kinases. Cell 82, 359–370.

Dütting, D., Handwerker, C., Drescher, U., 1999. Topographic targeting and pathfinding errors of retinal axons following overexpression of ephrinA ligands on retinal ganglion cell axons. Dev. Biol. 216, 297–311.

Eberhart, J., Swartz, M., Koblar, S.A., Pasquale, E.B., Tanaka, H., Krull, C.E., 2000. Expression of EphA4, ephrin-A2 and ephrin-A5 during axon outgrowth to the hindlimb indicates potential roles in pathfinding. Dev. Neurosci. 22, 237–250.

Eberhart, J., Swarz, M.E., Koblar, S.A., Pasquale, E.B., Krull, C.E., 2002. EphA4 constitutes a population-specific guidance cue for motor neurons. Dev. Biol. 247, 89–101.

Eberhart, J., Barr, J., O'Connell, S., Flagg, A., Swartz, M.E., Cramer, K.S., Tosney, K.W., Pasquale, E.B., Krull, C.E., 2004. Ephrin-A5 exerts

positic or inhibitory effects on distinct subsets of EphA4-positive motor neurons. J. Neurosci. 24, 1070–1078.
Fekete, D.M., Cepko, C.L., 1993. Replication-competent retroviral vectors encoding alkaline phosphatase reveal spatial restriction of viral gene expression/transduction in the chick embryo. Mol. Cell. Biol. 13, 2604–2613.
Frisen, J., Holmberg, J., Barbacid, M., 1999. Ephrins and their Eph receptors: multitalented directors of embryonic development. EMBO J. 18, 5159–5165.
Guidato, S., Prin, F., Guthrie, S., 2003. Somatic motoneurone specification in the hindbrain: the influence of somite-derived signals, retinoic acid and Hoxa3. Development 130, 2981–2996.
Hamburger, H., Hamilton, H., 1951. A series of normal stages in the development of the chick embryo. J. Morphol. 88, 49–92.
Helmbacher, F., Schneider-Maunoury, S., Topilko, P., Tiret, L., Charnay, P., 2000. Targeting of the EphA4 tyrosine kinase receptor affects dorsal/ventral pathfinding of limb motor axons. Development 127, 3313–3324.
Henrique, D., Adam, J., Myat, A., Chitnis, A., Lewis, J., Ish-Horowicz, D., 1995. Expression of a Delta homologue in prospective neurons in the chick. Nature 375, 787–790.
Higashijima, S., Hotta, Y., Okamoto, H., 2000. Visualization of cranial motor neurons in live transgenic zebrafish expressing green fluorescent protein under the control of the islet-1 promoter/enhancer. J. Neurosci. 20, 206–218.
Himanen, J.P., Chumley, M.J., Lackmann, M., Li, C., Barton, W.A., Jeffrey, P.D., Vearing, C., Geleick, D., Feldheim, D.A., Boyd, A.W., Henkemeyer, M., Nikolov, D.B., 2004. Repelling class discrimination: ephrin-A5 binds to and activates EphB2 receptor signaling. Nat. Neurosci. 5, 501–509.
Hornberger, M.R., Dütting, D., Ciossek, T., Yamada, T., Handwerker, C., Lang, S., Weth, F., Huf, J., Wessel, R., Logan, C., Tanaka, H., Drescher, U., 1999. Modulation of EphA receptor function by coexpressed ephrinA ligands on retinal ganglion cell axons. Neuron 22, 731–742.
Iwamasa, H., Ohta, K., Yamada, T., Ushijima, K., Terasaki, H., Tanaka, H., 1999. Expression of Eph receptor tyrosine kinases and their ligands in chick embryonic motor neurons and hindlimb muscles. Dev. Growth Differ. 41, 685–698.
Kania, A., Jessell, T.M., 2003. Topographic motor projections in the limb imposed by LIM homeodomain protein regulation of ephrin-A:EphA interactions. Neuron 38, 581–596.
Kania, A., Johnson, R.L., Jessell, T.M., 2000. Coordinate roles for LIM homeobox genes in directing the dorsoventral trajectory of motor axons in the vertebrate limb. Cell 102, 161–173.
Kilpatrick, T.J., Brown, A., Lai, C., Gassmann, M., Goulding, M., Lemke, G., 1996. Expression of the Tyro4/Mek4/Cek4 gene specifically marks a subset of embryonic motor neurons and their muscle targets. Mol. Cell. Neurosci. 7, 62–74.
Knöll, B., Drescher, U., 2002. Ephrin-As as receptors in topographic projections. Trends Neurosci. 25, 145–149.
Kullander, K., Klein, R., 2002. Mechanisms and functions of Eph and ephrin signaling. Nat. Rev., Mol. Cell Biol. 3, 475–486.
Kuratani, S., Tanaka, S., 1990. Peripheral development of avian trigeminal nerves. Am. J. Anat. 187, 65–80.
Küry, P., Gale, N., Connor, R., Pasquale, E., Guthrie, S., 2000. Eph receptors and ephrin expression in cranial motor neurons and the branchial arches of the chick embryo. Mol. Cell. Neurosci. 15, 123–140.
Lumsden, A., Keynes, R., 1989. Segmental patterns of neuronal development in the chick hindbrain. Nature 337, 424–428.
Marin, F., Puelles, L., 1995. Morphological fate of rhombomeres in quail/chick chimeras: a segmental analysis of hindbrain nuclei. Eur. J. Neurosci. 7, 1714–1738.
McClearn, D., Noden, D.M., 1988. Ontogeny of architectural complexity in embryonic quail visceral arch muscles. Am. J. Anat. 183, 277–293.
McLarren, K.W., Litsiou, A., Streit, A., 2003. DLX5 positions the neural crest and preplacode region at the border of the neural plate. Dev. Biol. 259, 34–47.
Momose, T., Tonegawa, A., Takeuchi, J., Ogawa, H., Umesono, K., Yasuda, K., 1999. Efficient targeting of gene expression in chick embryos by microelectroporation. Dev. Growth Differ. 41, 335–344.
Monschau, B., Kremoser, C., Ohta, K., Tanaka, H., Kaneko, T., Yamada, T., Handwerker, C., Hornberger, M.R., Loschinger, J., Pasquale, E.B., Siever, D.A., Verderame, M.F., Muller, B.K., Bonhoeffer, F., Drescher, U., 1997. Shared and distinct functions of RAGS and ELF-1 in guiding retinal axons. EMBO J. 16, 1258–1267.
Morgan, B.A., Fekete, D.M., 1996. Manipulating gene expression with replication-competent retroviruses. Methods Cell Biol. 51, 185–218.
Mueller, B.K., 1999. Growth cone guidance: first steps towards a deeper understanding. Annu. Rev. Neurosci. 22, 351–388.
Myat, A., Henrique, D., Ish-Horowicz, D., Lewis, J., 1996. A chick homologue of Serrate and its relationship with Notch and Delta homologues during central neurogenesis. Dev. Biol. 174, 233–247.
Nishida, K., Flanagan, J.G., Nakamoto, M., 2002. Domain-specific olivocerebellar projection regulated by the Eph–ephrinA interaction. Development 129, 5647–5658.
Noden, D.M., Marcucio, R., Borycki, A.G., Emerson Jr., C.P., 1999. Differentiation of avian craniofacial muscles: I. Patterns of early regulatory gene expression and myosin heavy chain synthesis. Dev. Dyn. 216, 96–112.
O'Leary, D.D., Wilkinson, D.G., 1999. Eph receptors and ephrins in neural development. Curr. Opin. Neurobiol. 9, 65–73.
Ohta, K., Nakamura, M., Hirokawa, K., Tanaka, S., Iwama, A., Suda, T., Ando, M., Tanaka, H., 1996. The receptor tyrosine kinase, Cek8, is transiently expressed on subtypes of motoneurons in the spinal cord during development. Mech. Dev. 54, 59–69.
Palmer, A., Klein, R., 2003. Multiple roles of ephrins in morphogenesis, neuronal networking, and brain function. Genes Dev. 17, 1429–1450.
Potts, W.M., Olsen, M., Boettiger, D., Vogt, V.M., 1987. Epitope mapping of monoclonal antibodies to gag protein p19 of avian sarcoma and leukaemia viruses. J. Gen. Virol. 68, 3177–3182.
Prince, V., Lumsden, A., 1994. Hoxa-2 expression in normal and transposed rhombomeres: independent regulation in the neural tube and neural crest. Development 120, 911–923.
Rosentreter, S.M., Davenport, R.W., Löschinger, J., Huf, J., Jung, J., Bonhoeffer, F., 1998. Response of retinal ganglion cell axons to striped linear gradients of repellent guidance molecules. J. Neurobiol. 37, 541–562.
Simon, H., Guthrie, S., Lumsden, A., 1994. Regulation of SC1/DM-GRASP during the migration of motor neurons in the chick embryo brainstem. J. Neurobiol. 25, 1129–1143.
Song, J., Boord, R.L., 1993. Motor components of the trigeminal nerve and organization of the mandibular arch muscles in vertebrates. Phylogenetically conservative patterns and their ontogenetic basis. Acta Anat. 148, 139–149.
Tucker, A., Lumsden, A., Guthrie, S., 1996. Cranial motor axons respond differently to the floor plate and sensory ganglia in collagen gel co-cultures. Eur. J. Neurosci. 8, 906–916.
Tsuchida, T., Ensini, M., Morton, S.B., Baldassare, M., Edlund, T., Jessell, T.M., Pfaff, S.L., 1994. Topographic organisation of embryonic motor neurons defined by expression of LIM homeobox genes. Cell 79, 957–970.
Varela-Echavarría, A., Pfaff, S.L., Guthrie, S., 1996. Differential expression of LIM homeobox genes among motor neuron subpopulations in the developing chick brainstem. Mol. Cell. Neurosci. 8, 242–257.
Vastrik, I., Eickholt, B.J., Walsh, F.S., Ridley, A., Doherty, P., 1999. Sema3A-induced growth-cone collapse is mediated by Rac1 amino acids 17–32. Curr. Biol. 9, 991–998.
Walkenhorst, J., Dütting, D., Handwerker, C., Huai, J., Tanaka, H., Drescher, U., 2000. The EphA4 receptor tyrosine kinase is necessary

for the guidance of nasal retinal ganglion cell axons in vitro. Mol. Cell. Neurosci. 16, 365–375.
Walter, J., Henke-Fahle, S., Bonhoeffer, F., 1987a. Avoidance of posterior tectal membranes by temporal retinal axons. Development 101, 909–913.
Walter, J., Kern-Veits, B., Huf, J., Stolze, B., Bonhoeffer, F., 1987b. Recognition of position-specific properties of tectal cell membranes by retinal axons in vitro. Development 101, 685–696.
Warrilow, J., Guthrie, S., 1999. Rhombomere origin plays a role in the specificity of cranial motor axon projections in the chick. Eur. J. Neurosci. 11, 1403–1413.
Wild, J.M., Zeigler, H.P., 1980. Central representation and somatotopic organisation of the jaw muscles within the facial and trigeminal nuclei of the pigeon (*Columba livia*). J. Comp. Neurol. 92, 175–201.
Wilkinson, D.G., Bhatt, S., Cook, M., Boncinelli, E., Krumlauf, R., 1989. Segmental expression of Hox-2 homoeobox-containing genes in the developing mouse hindbrain. Nature 341, 405–409.
Yue, Y., Chen, Z.Y., Gale, N.W., Blair-Flynn, J., Hu, T.J., Yeu, X., Cooper, M., Crockett, D.P., Yancopoulos, G.D., Tessarollo, L., Zhou, R., 2002. Mistargeting hippocampal axons by expression of a truncated Eph receptor. Proc. Natl. Acad. Sci. U. S. A. 99, 10777–10782.